Proceedings of the 20th International Conference on Soil Mechanics and Geotechnical Engineering– Rahman and Jaksa (Eds)

Permeability of materials used in the construction of a tailings dam

Perméabilité des matériaux utilisés dans la construction d'un barrage de résidus

Hernán Patiño
Colombian Institute of Geotechnical Researches, Colombia, director@icig.org.co

Rubén Galindo and Claudio Olalla
Polytechnic University of Madrid, Spain

ABSTRACT: In stages prior to the construction of tailings dam, one of the properties that must be investigated with precision is the hydraulic conductivity of the materials that will be used; so, this paper contains the results of 48 tests carried out on three materials used on the construction of the Riotinto tailings dam (Huelva - Spain). The equipment involved a modified triaxial system to facilitate the execution of permeability tests under constant head. The tests were performed on samples consolidated to 50, 100, 200, and 300 kPa, for four different hydraulic gradients established by applying a backpressure difference (ΔBp). The magnitude of the backpressure difference was applied as a percentage of the initial effective consolidation pressure, expressed as $\Delta Bp/\sigma'_c$, namely values of 10, 15, 20, and 25%. The backpressure (Bp) was constant (400 kPa) in all cases, allowing a degree of saturation close to 100% to be achieved. This was verified by calculating Skempton's B-parameter, which was very close to unity in all cases. The results indicate that it is feasible to define an empirical function including the coefficient of permeability (k) and the effective consolidation pressure (σ'_c), the mean effective confining pressure (σ'_{cav}) and the backpressure differential (ΔBp).

RÉSUMÉ : Dans les étapes préalables à la construction du barrage à résidus, l'une des propriétés qui doit être étudiée avec précision est la conductivité hydraulique des matériaux qui seront utilisés; ainsi, cet article contient les résultats de 48 essais effectués sur trois matériaux utilisés pour la construction du barrage de résidus Riotinto (Huelva - Espagne). L'équipement impliquait un système triaxial modifié pour faciliter l'exécution des essais de perméabilité à charge constante. Les essais ont été effectués sur des échantillons consolidés à 50, 100, 200 et 300 kPa, pour quatre gradients hydrauliques différents établis en appliquant une différence de contre-pression (ΔBp). L'amplitude de la différence de contre-pression a été appliquée en pourcentage de la pression de consolidation effective initiale, exprimée par $\Delta Bp/\sigma'_c$, à savoir 10, 15, 20 et 25%. La contre-pression (Bp) était constante (400 kPa) dans tous les cas, permettant d'atteindre un degré de saturation proche de 100%. Cela a été vérifié en calculant le paramètre B de Skempton, qui était très proche de l'unité dans tous les cas. Les résultats indiquent qu'il est possible de définir une fonction empirique incluant le coefficient de perméabilité (k) et la pression de consolidation effective ($\sigma'c$), la pression de confinement effective moyenne (σ'_{cav}) et le différentiel de contre-pression (ΔBp).

KEYWORDS: permeability; triaxial cell; skempton's B parameter; consolidation pressure; backpressure.

1 INTRODUCTION.

The investigation of aspects related to the permeability of earth materials has been of interest to practitioners of various disciplines, among which is the design and stability of earth dams.

The hydraulic conductivity of soils is usually determined by conducting variable or constant-head tests standardized by different specifications. These tests are performed with the use of equipment in which the specimen is confined by a rigid enclosure acting as a boundary along which water flows rather easily and therefore, the measured flow rate is not strictly equal to the volume passing through the sample. Taking this into account, the tests carried out as part of this investigation were executed using a triaxial system that was modified and adjusted as a permeameter with a flexible boundary, thus eliminating the effect of a rigid confining container. The tests carried out are not standardized, because the equipment used was developed at the Polytechnic University of Madrid in Spain, to guarantee the sample full saturation, with the simultaneous application of water pressure at the bottom and vacuum at the top drainage. This allows the saturation of the specimens through the application of backpressure. In addition, a double pressure system ensured that the hydraulic gradient kept a constant value throughout the test. Once the equipment was tuned, it allowed the possibility of performing tests under different effective consolidation pressures.

The interest in studying the validity of Darcy's Law, the fundamental aspects of soil permeability, and the factors governing the magnitude of the coefficient of permeability (k) are reflected in investigations performed by (Kozeny 1927, Taylor 1948, Carman 1956, Mesri and Olson 1971, Remy 1973, Tavenas et al. 1983ab, Witt and Brauns 1983, Daniel et al. 1984, Kenney et al. 1984, Carpenter and Stephenson 1986, Fukushima and Ishii 1986, Chapuis et al. 1989, Uppot and Stephenson 1989, Budhu et al. 1991, Hatanaka et al. 1997, Olalla and Cuéllar 1998, Cortellazzo et al. 2001, Sridharan et al. 2002, Carrier 2003, Chapuis and Aubertin 2003, Setiano et al. 2003, Wong 2003, Sathananthan and Indraratna 2006, Zhang et al. 2012, Ozgumus et al. 2014, Martínez 2107, Ranivomanana et al. 2017 and Patiño et al. 2019).

The objective of the new investigation presented herein is to disclose the results of permeability tests carried out with a triaxial system modified by us so as to guarantee the saturation of the specimens, The new test method consists in removing all the air trapped in the system, by applying vacuum through the upper drainage of the specimen and simultaneously allowing the slow entry of de-aerated water through the lower drainage.

The way to apply backpressure at the top and bottom of the specimen makes it possible to maintain the hydraulic gradient at constant levels during all the time necessary for the execution of the tests. The results of the permeability tests reported in this paper constitute part of a more comprehensive investigation aimed at evaluating the geotechnical behavior of mine tailings focused on verifying the stability, under both static and dynamic conditions, of earth dams built with these types of materials.

2 DESCRIPTION OF THE TESTED MATERIALS

The samples used in this investigation were recovered from tailing deposits resulting from mining activities at the Riotinto mines near Huelva, in the Southwest of Spain. The mines concentrate the most important deposits of gold, copper, and silver in the country. Historically, the inhabitants of the region have depended on the mines for over 4000 years; it has been found that these deposits attracted the first settlers to the region as far back as 2000 BC. Excavations at the Riotinto mines have generated, within an area of about 1200 hectares, a large number of mine dumps and tailing dams that, under present conditions, are sources of geotechnical interest, mainly in relation to their stability and seepage conditions. Figure 1 shows a sketch profile of Riotinto tailings dam.

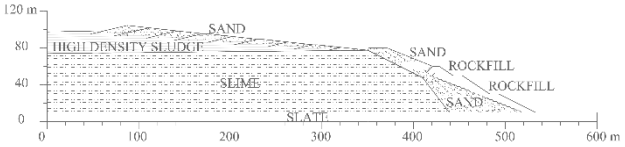

Figure 1. Sketch profile of Riotinto tailings dam

The samples that were used were recovered superficially from the dam itself. The three materials to be referred to are identified at the mine site as: "*Cerro Salomón* sand" - CSS (Greenish-gray, fine-grained, silty sand), "high density sludge" - HDS (Greenish-gray, fine-grained), and "copper *lamas*" - CL) (Ochre silty clay). The information related to the index properties of the three materials tested is contained in Table 1.

Further details on the *Riotinto* tailings dam can be obtained by consulting the work of (Martínez 2017).

Table 1. Properties and mineralogy of materials tested.

Propertie	Unit	Material		
		CSS	HDS	CL
Natural moisture	%	8.1	14	38.5
Lab. Moisture	%	8.1	7.8	25
Particle size <80 µm	%	32.7	49	85.9
Liquid limit, LL	%			26.9
Plastic limit, PL	%			19.9
Plasticity index, PI	%	NP	NP	7
Specific gravity		3.02	3	2.83
Dry density, γ_d	g/cm^3	1.6	1.7	1.65
Initial void ratio, e_o		0.89	0.8	0.72
Quartz	%	92	82	23
Chlorite	%			50
Mica	%	8	6	17
Pyrite	%			10
Jarosite	%		12	

3 DESCRIPTION OF THE EQUIPMENT USED

The equipment that was used to perform the tests included a modified triaxial system in which, similar to conventional triaxial compression tests, the specimen is protected by a latex membrane. The modified system allows application of different backpressures at the upper and lower ends of the specimen. Normally triaxial systems are equipped with a double pressure system; one, to apply the cell pressure; and the other, to apply a homogenous backpressure through the lower and upper drainages of the samples, which does not generate flow, except in the consolidation stage. To perform permeability tests in triaxial cells, the authors implemented an additional pressure system designed to apply a greater back pressure through the lower drainage of the specimen (with respect to that applied at the upper drainage). Under these conditions, upward flow is generated through the specimen and, therefore, the permeability test can be performed. Figure 2 shows a schematic representation of the specimens during the permeability tests. Further details on the equipment used can be obtained by consulting the works of (Martínez 2017) and (Patiño et al. 2019).

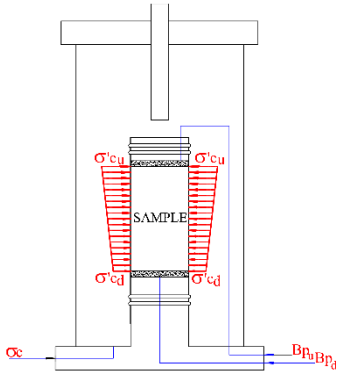

Figure 2. Sample conditions during permeability tests.

4 EXPERIMENTAL PROGRAM

For each of the three materials that were investigated, 16 permeability tests were performed. During the consolidation stage of each test, the total pressures applied (σ_c) were equal to 450, 500, 600, and 700 kPa and the backpressure (Bp) was equal to 400 kPa. Considering that:

$$\sigma'_c = \sigma_c - Bp \quad (1)$$

Where σ'_c is the effective pressure during the consolidation stage, σ_c is the cell pressure during the consolidation stage and Bp is the backpressure during the consolidation stage.

The effective pressure (σ'_c) during the consolidation stage was equal to 50, 100, 200, and 300 kPa.

The differences between the backpressures applied to the top and bottom of the specimens (ΔBp) were equal to 10, 15, 20, and 25% of each of the effective consolidation pressures applied; hydraulic gradients ranging from 5 to 80 were obtained for the different combinations.

During the execution of the permeability tests in the triaxial cell, differences exist between the backpressures applied at the upper and lower ends of the specimens and the effective confining stress varies linearly from a low value at the base to a high value at the top If this is taken into account, the term "mean effective confining pressure" (σ'_{cav}) can be introduced and is defined by means of expression (2).

$$\sigma'_{cav} = \sigma_c - \left\{\frac{B_{pu} + B_{pd}}{2}\right\} \quad (2)$$

Where σ_c is the cell pressure, Bp_u is the backpressure applied by the upper drainage and Bp_d is the backpressure applied by the lower drainage

To facilitate interpretation of the results, special care was taken to maintain the different values of the ratio $\Delta Bp/\sigma'_c$ for the different values of σ'_c at a constant level, as observed in Table 2, i.e., the values are equal to 10, 15, 20 and 25%.

The general conditions under which the tests were carried out are summarized in Table 2. In all tests, the value of Skempton' B-parameter ranged between 0.992 and 0.997.

4 RESULTS

The results of the 48 permeability tests that were carried out are reported in Table 3.

Table 2. General conditions of the tests carried out on each material.

Consolidation			Permeability tests					
σ_c	Bp	σ'_c	Bp_u	Bp_d	ΔBp	$\Delta Bp/\sigma'_c$	Bp_{av}	σ'_{cav}
kPa	kPa	kPa	kPa	kPa	kPa	%	kPa	kPa
450	400	50	400	405	5	10	402.5	47.5
				408	7.5	15	403.8	46.3
				410	10	20	405	45
				413	12.5	25	406.3	43.8
500	400	100	400	410	10	10	405	95
				415	15	15	407.5	92.5
				420	20	20	410	90
				425	25	25	412.5	87.5
600	400	200	400	420	20	10	410	190
				430	30	15	415	185
				440	40	20	420	180
				450	50	25	425	175
700	400	300	400	430	30	10	415	285
				445	45	15	422.5	278
				460	60	20	430	270
				475	75	25	437.5	263

In what follows, charts are presented to depict the trends in the variation of the coefficient of permeability (k), as a function of the mean effective confining pressure (σ'_{cav}) as well as the permeability as a function of the backpressure differential (ΔBp) applied to the top and bottom of the specimens, normalized with respect to the effective consolidation pressure (σ'_c).

Figure 3 shows, for each of the materials, four sets of variation trends of the permeability as a function of the mean effective confining pressure (σ'_{cav}) although in this case for four different values of $\Delta Bp/\sigma'_c$ equal to, from top to bottom, 10, 15, 20, and 25%.

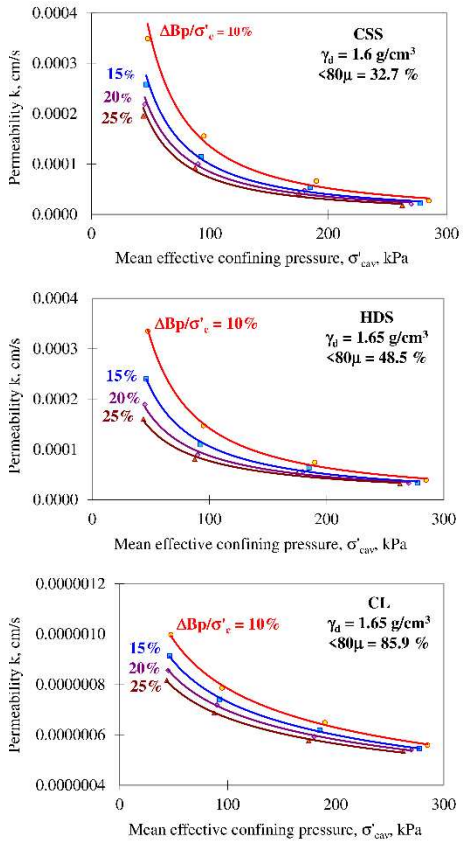

Figure 3. Variation trends of the coefficient of permeability as a function of the mean effective confining pressure, for different ratios $\Delta Bp/\sigma'_{cav}$.

Taking into account the information contained in Figure 3 the following results were obtained:

- Regardless of the type of material and the ratio $\Delta Bp/\sigma'_c$, the permeability tends to decrease when the mean effective confining pressure is increased.
- For equal values of the mean effective confining pressure the permeability tends to decrease when the ratio $\Delta Bp/\sigma'_c$ is increased.
- For the different values of the ratio $\Delta Bp/\sigma'_c$ it is possible to determine empirical power functions between the coefficient of permeability and the mean effective confining pressure through the use of equation (3), in all cases with regression coefficients $R^2 > 0.98$.

$$k = a \cdot (\sigma'_{cav})^b \tag{3}$$

Where k is the coefficient of permeability in cm/s, a and b are empirical constants, included in Table 4, and σ'_{cav} is the mean effective confining pressure in kPa.

If the empirical power functions for each material are used, it is possible to plot the graphs shown in Figure. 4 where the coefficient of permeability is correlated to the ratio $\Delta Bp/\sigma'_c$, for different values of the mean effective confining pressure, in this case equal to 50, 100, 150, 200, 250, and 300 kPa.

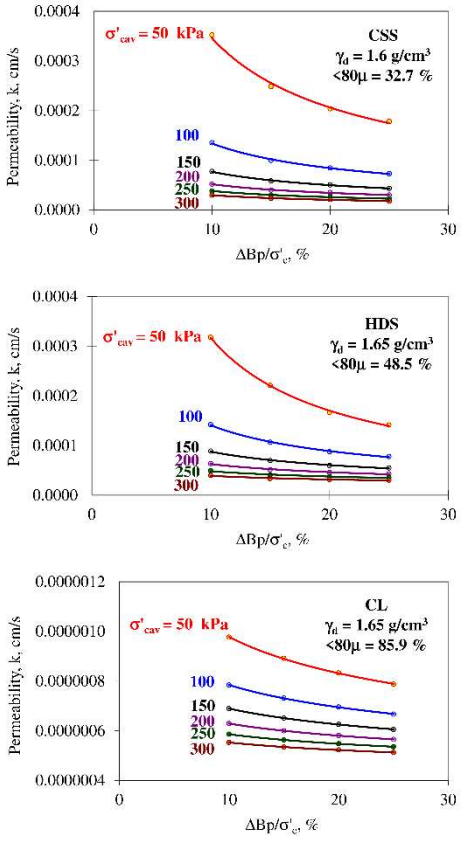

Figure 4. Variation trends of the coefficient of permeability as a function of the ratio $\Delta Bp/\sigma'_c$, for different values of mean effective consolidation pressure σ'_{cav}.

Based on the information contained in Figure 4 the following results can be derived:

- Regardless of the type of material and of the mean effective confining pressure, the permeability tends to decrease when the ratio $\Delta Bp/\sigma'_c$ is increased. In turn, this influence tends to be negligible when the mean effective confining pressure is increased.

Table 3. Results of the permeability test .

Consolidation			Permeability tests												
								CSS			HDS			CL	
σ_c	Bp	σ'_c	Bp_d	Bp_{av}	σ'_{cav}	ΔBp	ΔBp/σ'_c	i	q	k	i	q	k	i	q	k
kPa	kPa	kPa	kPa	kPa	kPa	kPa	%		cm^3/s	cm/s		cm^3/s	cm/s		cm^3/s	cm/s
450	400	50	405	403	47.5	5	10	4.87	0.03	3.49E-04	4.93	0.03	3.35E-04	4.57	9E-05	.1.02E-07
450	400	50	408	404	46.3	7.5	15	7.3	0.04	2.58E-04	7.4	0.04	2.40E-04	6.85	0.0001	9.14E-07
450	400	50	410	405	45	10	20	9.74	0.04	2.19E-04	9.86	0.04	1.89E-04	9.13	0.0002	8.56E-07
450	400	50	413	406	43.8	12.5	25	12.2	0.05	1.95E-04	12.3	0.04	1.60E-04	11.4	0.0002	8.16E-07
500	400	100	410	405	95	10	10	9.76	0.03	1.56E-04	9.96	0.03	1.47E-04	9.18	0.0001	7.86E-07
500	400	100	415	408	92.5	15	15	14.6	0.03	1.15E-04	14.9	0.03	1.09E-04	13.8	0.0002	7.41E-07
500	400	100	420	410	90	20	20	19.5	0.04	1.00E-04	19.9	0.04	8.92E-05	18.4	0.0003	7.19E-07
500	400	100	425	413	87.5	25	25	24.4	0.04	9.22E-05	24.9	0.04	8.09E-05	23	0.0003	6.87E-07
600	400	200	420	410	190	20	10	19.6	0.03	6.62E-05	20.4	0.03	7.45E-05	18.9	0.0003	6.49E-07
600	400	200	430	415	185	30	15	29.4	0.03	5.37E-05	30.6	0.04	6.37E-05	28.4	0.0004	6.18E-07
600	400	200	440	420	180	40	20	39.1	0.04	4.77E-05	40.9	0.05	5.59E-05	37.9	0.0005	5.93E-07
600	400	200	450	425	175	50	25	48.9	0.04	4.25E-05	51.1	0.05	5.22E-05	47.4	0.0005	5.76E-07
700	400	300	430	415	285	30	10	29.7	0.02	2.72E-05	32.7	0.03	3.94E-05	30.4	0.0004	5.59E-07
700	400	300	445	423	278	45	15	44.6	0.02	2.20E-05	49	0.03	3.33E-05	45.6	0.0005	5.44E-07
700	400	300	460	430	270	60	20	59.4	0.02	2.06E-05	65.4	0.05	3.31E-05	60.9	0.0007	5.40E-07
700	400	300	475	438	263	75	25	74.3	0.03	1.79E-05	81.7	0.06	3.21E-05	76.1	0.0009	5.35E-07

- For the different values of the mean effective confining pressure it is also possible to establish power functions between the coefficient of permeability and the ratio ΔBp/σ'$_c$ through the use of expression (4), in all cases with regression coefficients $R^2 > 0.98$.

$$k = c \cdot \left(\frac{\Delta Bp}{\sigma'_c}\right)^d \quad (4)$$

Where k is the coefficient of permeability in cm/s, c and d are empirical constants, included in Table 4, σ'$_c$ is the effective consolidation pressure in kPa, ΔBp = Bpd - Bpu in kPa, and the ratio ΔBp/σ'$_c$ is in percentage.

Table 4. Values of the constants in the empirical functions (3) and (4).

CSS					
ΔBp/σ'$_c$, %	a	b	σ'$_{cav}$, kPa	c	d
10	0,078	-1,380	50	0,0019	-0,749
15	0,043	-1,319	100	0,0006	-0,671
20	0,029	-1,270	150	0,0003	-0,626
25	0,027	-1,288	200	0,0002	-0,593
			250	0,0001	-0,568
			300	0,0001	-0,548
CL					
ΔBp/σ'$_c$, %	a	b	σ'$_{cav}$, kPa	c	d
10	0,0000034	-0,317	50	0,0000017	-0,235
15	0,0000027	-0,286	100	0,0000012	-0,176
20	0,0000023	-0,260	150	0,0000010	-0,141
25	0,0000020	-0,240	200	0,0000008	-0,117
			250	0,0000007	-0,098
			300	0,0000007	-0,082
HDS					
ΔBp/σ'$_c$, %	a	b	σ'$_{cav}$, kPa	c	d
10	0,030	-1,162	50	0,00250	-0,897
15	0,014	-1,053	100	0,00065	-0,665
20	0,006	-0,932	150	0,00030	-0,530
25	0,004	-0,861	200	0,00017	-0,434
			250	0,00011	-0,359
			300	0,00008	-0,299

From the data included in Table 4, for each of the materials, it is possible to establish a function including the constants c and d and the mean effective confining pressure in order to determine a more general function correlating the coefficient of permeability with the three factors that vary during the execution of the permeability tests using the triaxial cell, namely: the effective consolidation pressure (σ'$_c$), the mean effective confining pressure (σ'$_{cav}$), and the ratio ΔBp/σ'$_c$.

Constants c and d can be correlated with the mean effective confining pressure through the use of the empirical functions (5), Figure 5, and (6), Figure 6. Among the most used, the functions with the highest regression coefficient R^2 were chosen.

$$c = f \cdot (\sigma'_{cav})^g \quad (5)$$

$$d = h \cdot ln(\sigma'_{cav}) + j \quad (6)$$

Substituting c and d in expression (4) for the empirical functions (5) and (6), the general empirical equation (7) is obtained which correlates the coefficient of permeability with the three factors that are variables during the execution of the permeability tests using a triaxial cell.

$$k = f \cdot (\sigma'_{cav})^g \cdot \left\{\frac{\Delta Bp}{\sigma'_c}\right\}^{h \cdot \ln \cdot (\sigma'_{cav}) + j} \quad (7)$$

Where f, g, h and j are empirical constants, included in Table 5, k is the coefficient of permeability in cm/s, σ'$_{cav}$ is the mean effective confining pressure in kPa and the ratio ΔBp/σ'$_c$ is in percentage.

Table 5. Values of the constants in the empirical function (7).

Material	% fines	Average void ratio	f	g	h	j
CSS	32.7	0.88	1.1	-1.63	0.11	-1.2
CL	85.9	0.70	0.000013	-0.52	0.085	-0.57
HDS	48.5	0.78	4.9	-1.94	0.334	-2.2

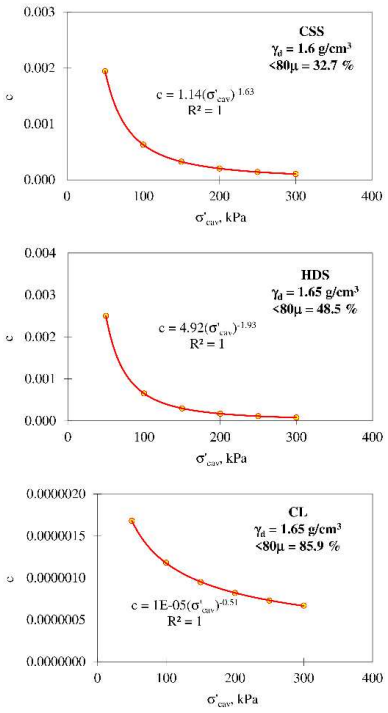

Figure 5. Variation trends of constant c as a function of mean effective consolidation pressure σ'_{cav}.

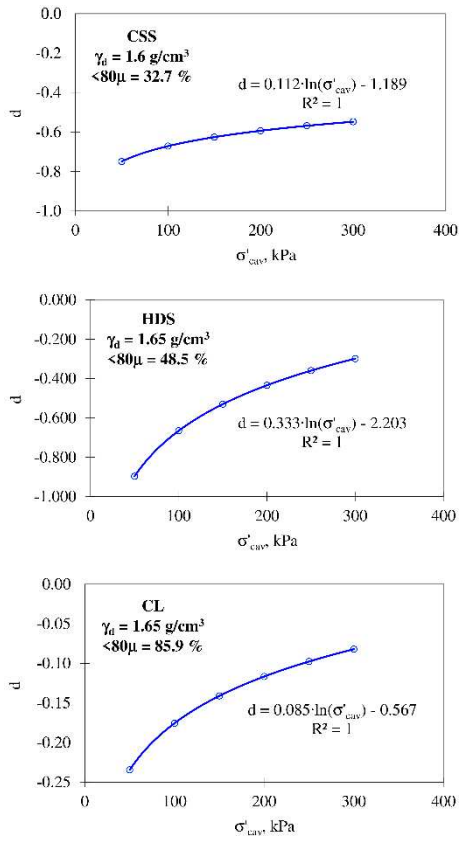

Figure 6. Variation trends of constant d as a function of mean effective consolidation pressure σ'_{cav}.

For purposes of visualizing the accuracy with which the empirical functions reproduce the data obtained from the permeability tests executed in the laboratory using the triaxial cell, Figure 7 was plotted to include all of the experimental results and, with larger points, the values generated by the empirical function. Figure 7 shows larger points in the CSS material for a pressure of 300 kPa; in the HDS material for a pressure of 50 kPa, and in the CL material for a pressure of 100 kPa.

As already mentioned, this research was oriented to characterize the behavior of materials from the actual Riotinto tailings dam, which were placed under certain density (or void ratio) conditions. The work has shown that in-situ sample densities were high; consequently the consolidation pressure that was later applied could reduce the sample void ratios only very slightly. Even though this parameter varies very little, attempts have been done to relate the permeability coefficient with the void ratio (Patiño 2019).

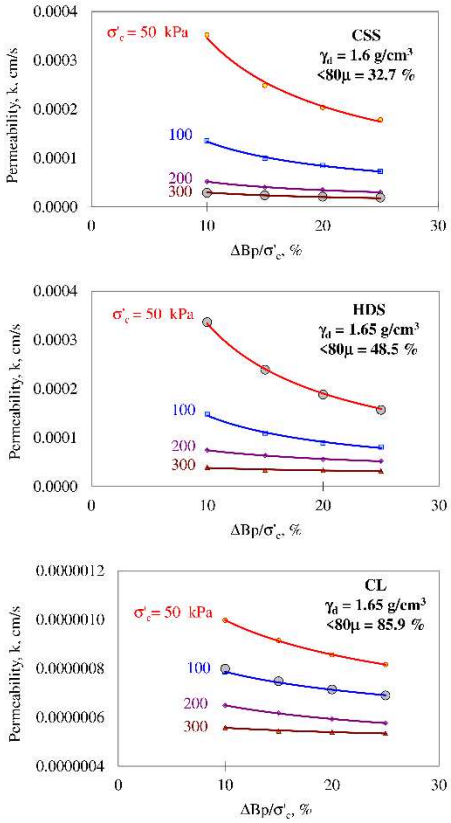

Figure 7. Variation trends of the coefficient of permeability as a function of the ratio $\Delta Bp/\sigma'_c$, for different values of mean effective consolidation pressure σ'_c. The solid lines correspond to the experimental data and the larger points to the values generated by the empirical functions.

5 CONCLUSIONS

This article studies the permeability of mine tailings actually employed to build a number of dams. For this reason, the fines content and void ratio values have been practically constant for all samples tested that correspond to the same material. The main conclusions of this study are summarized as follows:

- In triaxial cells, it is very convenient to implement an inundation phase prior to the usually known as saturation phase. Applying vacuum to extract the air trapped in the system facilitates the solution in water of the air exclusively contained in the sample voids. This procedure guarantees a degree of saturation near 100%.
- Mine tailings exhibit a permeability behaviour similar to that of more conventional materials. Fines content is the most conditioning factor in the permeability coefficient.
- For the CL material, with a fines content of 85%, the permeability coefficient is nearly independent of gradient and consolidation pressure. It ranges from $6x10^{-7}$ to $10x10^{-7}$ cm/s, and consequently that variation is little significant in practice.

Therefore, only a very low number of tests would be required to estimate the permeability coefficient of this material

- Regardless of the material, the increase in the ratio $\Delta Bp/\sigma'c$ entails a reduction of the permeability but, as the effective consolidation pressure increases, the effect of a higher $\Delta Bp/\sigma'c$ ratio tends to be lower, and negligible in the case of material CL.
- A simple empirical function is proposed to correlate the coefficient of permeability (k) with the effective consolidation pressure (σ'_c), the mean effective confining pressure (σ'_{cav}) and the backpressure differential (ΔBp).
- The authors think that the functions proposed could be extrapolated to samples presenting comparable fines content and void ratio values. If these variables are different, it would suffice to test a limited number of samples (nine) to estimate the law of variation of the permeability coefficient. From this work it can be deduced that, for the same material, the permeability coefficient decreases as the consolidation pressure increases. This variation can be introduced in seepage and stability calculations via the expressions suggested in the article.

6 ACKNOWLEDGEMENTS

The *Fundación José Entrecanales Ibarra* is acknowledged for their support in the form of funds to purchase the equipment, and the *EPTISA Servicios de Ingeniería* for sponsoring the investigation.

7 REFERENCES

Budhu M., Giese R.F. Jr., Campbell G. and Baumgrass L. 1991. The permeability of soils with organic fluids. Canadian Geotechnical Journal, **28**(1): 140-147. http://dx.doi.org/10.1139/t91-015.

Carman P.C. 1956. Flow of gases through porous media. Butterworths, London.

Carpenter G.W. and Stephenson R.W. 1986. Permeability Testing in the Triaxial Cell. Geotechnical Testing Journal, **9**(1): 3-8.

Chapuis R. and Aubertin M. 2003. Predicting the coefficient of permeability of soils using the Kozeny-Carman equation. Department CGM, École Polytechnique de Montréal. http://dx.doi.org/10.1139/t89-074.

Chapuis R., Gil D. and Baass K. 1989. Laboratory permeability tests on sand: influence of the compaction method on anisotropy. Canadian Geotechnical Journal, **26**(4): 614-622.

Cortellazzo G. and Simonini P. 2001. Permeability evaluation and its implications for consolidation analysis of an Italian soft clay deposit. Canadian Geotechnical Journal, **38**(6): 1166-1176. http://dx.doi.org/10.1139/t01-042.

Daniel D., Trautwein S., Boynton S. and Foreman D. 1984. Permeability Testing with Flexible-Wall Permeameters. Geotechnical Testing Journal, **7**(3): 113-122.

Fukushima S. and Ishii T. 1986. An experimental study of the influence of confining pressure on permeability coefficients of fill dam core material. Soils and Foundations, **26**(4): 32-46.

Hatanaka M., Uchida A. and Takehara N. 1997. Permeability Characteristics of High –Quality Undisturbed Sands Measured in a Triaxial Cell. Soils and Foundations, **37**(3): 129-135. http://dx.doi.org/10.3208/sandf.37.3_129.

Kenney T.C., Lau D. and Ofoegbu G.I. 1984. Permeability of compacted granular materials. Canadian Geotechnical Journal, **21**(4): 726-729. http://dx.doi.org/10.1139/t84-080.

Kozeny J. 1927. Ueber kapillare Leitung des Wassers im Boden. Sitzungsber Akad. Wiss, Wien, **136**(2a): 271-306.

Martínez E. 2017. Propiedades geotécnicas de los estériles mineros de las minas de Riotinto, Huelva – España. [PhD Thesis]. Escuela Técnica Superior de Ingenieros de Caminos, Canales y Puertos. Universidad Politécnica de Madrid. España.

Mesri G. and Olson R. E. 1971. Mechanisms controlling the permeability of clays. Clays and Clay Minerals, 19: 151-158.

Olalla C. and Cuéllar V. 1998. Estudio del mecanismo de rotura de la presa de Aznalcollar. Informe técnico del Centro de Estudios y Experimentación de Obras Públicas – CEDEX, Tomo I. España.

Ozgumus T., Mobedi M. and Ozkol U. 2014. Determination of Kozeny constant based on porosity and pore to throat size ratio in porous medium with rectangular rods. Engineering Applications of Computational Fluid Mechanics, **8**(2): 308–318. http://dx.doi.org/10.1080/19942060.2014.11015516.

Patiño H., Martínez E., González J and Soriano A. 2019. Permeability of mine tailings measured in triaxial cell. Can. Geotech. J., Volume 56, number 4, 587-599. https://doi.org/10.1139/cgj-2017-0293

Ranaivomanana H., Razakamanantsoa A. and Amiri O. 2017. Permeability Prediction of Soils Including Degree of Compaction and Microstructure. Journal of Geomechanics, **17**(4). http://dx.doi.org/10.1061/(ASCE)GM.1943-5622.0000792.

Remy J.I. 1973. The measurement of small permeabilities in the laboratory. Geotechnique, 3(3): 454-458.
http://dx.doi.org/10.1680/geot.1973.23.3.454.

Sathananthan I. and Indraratna B. 2006. Laboratory Evaluation of Smear Zone and Correlation between Permeability and Moisture Content. Journal of Geotechnical and Geoenvironmental Engineering, 132(7): 942-945.
http://dx.doi.org/10.1061/(ASCE)1090-0241(2006)132:7(942).

Setianto A., Leong, E. and Rahardjo H. 2003. A flexible wall permeameter for measurements of water and air coefficients of permeability of residual soils. Canadian Geotechnical Journal, **40**(3): 559-574.

Sridharan A. and Prakash K. 2002. Permeability of Two-Layer Soils. Geotechnical Testing Journal, 25(4): 443-448.

Tavenas F., Leblond P., Jean P. and Leroueil S. 1983a. The Permeability of Natural Soft Clays, Part I. Methods of Laboratory Measurement. Canadian Geotechnical Journal, **20**(4): 629-644.
http://dx.doi.org/10.1139/t83-072.

Tavenas F., Leblond P., Jean P. and Leroueil, S. 1983b. The Permeability of Natural Soft Clays, Part II. Permeability Characteristics. Canadian Geotechnical Journal, **20**(4): 645-660. http://dx.doi.org/10.1139/t83-072.

Uppot J. and Stephenson R. 1989. Permeability of Clays under Organic Permeants. Journal of Geotechnical Engineering, **115**(1): 115-131. http://dx.doi.org/10.1061/(ASCE)0733-9410(1989)115:1(115).

Taylor D. W. 1948. Fundamentals of soil mechanics. John Wiley & Sons Inc., New York, 700p. http://dx.doi.org/10.1097/00010694-194808000-00008.

Witt K. and Brauns J. 1983. Permeability-Anisotropy Due to Particle Shape. Journal of Geotechnical Engineering, 109(9): 1181-1187. http://dx.doi.org/10.1061/(ASCE)0733-9410(1983)109:9(1181).

Wong R. 2003. A model for strain-induced permeability anisotropy in deformable granular media. Canadian Geotechnical Journal, **40**(1): 95-106. http://dx.doi.org/10.1139/t02-088.

Zhang L., Aziz N., Ren T., Nemcik J. and Wang, Z. 2012. Permeability testing of coal under different triaxial conditions, 12th Coal Operators' Conference, University of Wollongong & The Australasian Institute of Mining and Metallurgy, pp. 277-285.